Original Article

J Korean Soc Radiol 2023;84(1):253-262
https://doi.org/10.3348/jksr.2022.0008
eISSN 2951-0805

JOURNAL of THE KOREAN SOCIETY of RADIOLOGY

Clinicoradiological Features of Pulmonary Cryptococcosis in Immunocompetent Patients

정상 면역 환자에서 폐 크립토코쿠스증의 임상방사선학적 특징

Hong Seok Choi, MD[1], Yun-Hyeon Kim, MD[1,2*], Won Gi Jeong, MD[3], Jong Eun Lee, MD[1], Hye Mi Park, MD[1]

[1]Department of Radiology, Chonnam National University Hospital, Gwangju, Korea
[2]Department of Radiology, Chonnam National University Medical School, Gwangju, Korea
[3]Department of Radiology, Chonnam National University Hospital, Hwasun, Korea

ORCID iDs
Hong Seok Choi https://orcid.org/0000-0003-2421-1091
Yun-Hyeon Kim https://orcid.org/0000-0002-0047-0729
Won Gi Jeong https://orcid.org/0000-0003-2821-2788
Jong Eun Lee https://orcid.org/0000-0002-8754-6801
Hye Mi Park https://orcid.org/0000-0002-9920-3400

Received January 13, 2022
Revised June 28, 2022
Accepted July 20, 2022

***Corresponding author**
Yun-Hyeon Kim, MD
Department of Radiology,
Chonnam National University Hospital,
Chonnam National University Medical School,
42 Jebong-ro, Dong-gu,
Gwangju 61469, Korea.

Tel 82-62-220-5747
Fax 82-62-226-4380
E-mail yhkim001@jnu.ac.kr

Purpose To assess the clinicoradiological features of pulmonary cryptococcosis in immunocompetent patients.

Materials and Methods This retrospective study included immunocompetent patients who had been diagnosed with pulmonary cryptococcosis on the histopathologic exam and underwent chest CT between January 2008 and November 2019. Imaging features were divided into major imaging patterns, distributions, and ancillary imaging findings. Univariable analysis was performed to evaluate clinicoradiological features according to the presence of serum cryptococcal antigen.

Results Thirty-one patients were evaluated (mean age: 60 years, range: 19–78 years). A single nodular lesion confined to a single lobe was the most common imaging pattern (14/31, 45.2%). Serum cryptococcal antigen tests were performed in 19 patients (19/31, 61.3%). The presence of serum cryptococcal antigen was observed in six patients (6/19, 31.6%), all of whom showed a consolidation-dominant pattern. The presence of serum cryptococcal antigen was significantly associated with the consolidation-dominant pattern compared to those associated with a nodule-dominant pattern ($p = 0.011$).

Conclusion A combination of CT findings of consolidation and a positive serum cryptococcal antigen test may be helpful for diagnosing pulmonary cryptococcosis in immunocompetent patients.

Index terms Immunocompetence; Cryptococcosis; Lung; Multidetector Computed Tomography

JOURNAL of THE KOREAN SOCIETY of RADIOLOGY

INTRODUCTION

The genus *Cryptococcosis* is a ubiquitous encapsulated yeast-like fungus and may cause pulmonary infection through inhalation of fungal spores. Though pulmonary cryptococcosis is common in immunocompromised patients with impairment of T-cell mediated immunity, it has also become an emerging disease in immunocompetent patients (1). The common radiologic features of pulmonary cryptococcosis have been largely classified into the following three patterns: a solitary nodule or mass, mass-like consolidation, or reticulonodular patterns. Cavitation, lymphadenopathy, and pleural effusion are also known as additional manifestations of the condition on CT scans (2, 3). Although the radiologic manifestation of pulmonary cryptococcosis is well-documented, diagnosis of pulmonary cryptococcosis is still challenging, especially in immunocompetent patients, as patients usually present with nonspecific clinical symptoms and radiologic manifestations (4, 5). Furthermore, the manifestation of pulmonary cryptococcosis in immunocompetent patients is complex as they usually show localized nodular lesions on CT scans that make them difficult to differentiate from malignancy (6-8).

Recently, serum cryptococcal antigen (CrAg) test using serum and cerebrospinal fluid has been widely used as a fast and sensitive test and has been drawing attention as an emerging tool in diagnosing pulmonary cryptococcosis (1, 9).

The purpose of this study was to assess the clinicoradiologic features of pulmonary cryptococcosis in immunocompetent patients.

MATERIALS AND METHODS

This study was approved by the Institutional Review Board of Chonnam National University Hospital (IRB No. CNUH-2021-440). The requirement for informed consent was waived due to the study's retrospective design.

PATIENTS

This retrospective study included 31 patients histologically diagnosed with pulmonary cryptococcosis after undergoing chest CT at the Chonnam National University Hospital from January 2008 to November 2019. No patient had any one of the following conditions: underlying hematologic malignancy, use of immunosuppressant drugs, uncontrolled diabetes mellitus, or HIV infection. The medical records of all patients, including their demographics, comorbidities, presenting symptoms, and laboratory test results, were collected.

DIAGNOSIS OF PULMONARY CRYPTOCOCCOSIS

The diagnosis of pulmonary cryptococcosis was confirmed by histologic evidence of the organism in the lung biopsy specimens. All samples were fixed with conventional 4% neutral formalin, embedded in paraffin, stained with hematoxylin-eosin, periodic acid-Schiff, mucicarmine, and Grocott's methenamine silver. CrAg tests were performed with a kit (Pastorex Crypto Plus, Bio-RAD, Marnes-la-Coquette, France) using the latex agglutination technique.

CT PROTOCOL

Chest CT scans were performed in all patients within 1 month prior to biopsy. Helical CT scans were acquired on a variety of multidetector row scanners using 16-slice (LightSpeed 16, GE Healthcare, Waukesha, WI, USA; SOMATOM scope, Siemens Medical Solutions, Forchheim, Germany), 64-slice (LightSpeed VCT, GE Healthcare; Discovery 750HD, GE Healthcare), dual-source 128-slice (SOMATOM definition flash, Siemens Medical Solutions), and 256-slice (Revolution CT, GE Healthcare) CT scanners. Contrast-enhanced images were routinely obtained in all patients. The slice thickness of high-resolution CT scans was 2–3 mm.

IMAGE ANALYSIS

Imaging features included major imaging patterns, distributions, and ancillary imaging findings on CT scans. Major imaging patterns included nodule-dominant and consolidation-dominant patterns. Distributions were divided into single vs. multi-lobar, upper vs. non-upper, and peripheral vs. central locations. Ancillary imaging findings included ground-glass opacity components, air bronchograms, cavitation, pleural tagging, pleural effusion, mediastinal lymphadenopathy, degree of enhancement on post-contrast CT scans, and maximum standardized uptake value (SUVmax) on ^{18}fluorodeoxyglucose (FDG)-PET/CT. Consolidation, ground-glass opacities, air bronchograms, and cavitation were defined according to the recommendations of the Nomenclature Committee of the Fleischner Society (10).

Nodules were defined as round or oval opacities that were at least moderately demarcated, regardless of size. If the lung lesions consisted mainly of nodules, they were classified as a nodular-dominant pattern, and if they were mainly consolidation, they were classified as a consolidation-dominant pattern. In the case of a nodular-dominant pattern, it was divided into single nodular, clustered nodular, and scattered nodular patterns. The single nodular pattern was defined as when the lesion consisted of a single nodule. The pattern was classified as clustered nodular if the lesion consisted of multiple nodules confined to one lobe, whereas the pattern was classified as scattered nodular if the lesion consisted of multiple nodules and were distributed over several lobes. The consolidation dominant pattern was also divided into single lobar and multi-lobar consolidations depending on whether the lesions were confined to a single lobe or not.

The distribution was determined according to the overall involvement and the location of the dominant lesion. The craniocaudal distribution was divided into upper and non-upper distributions, while the axial distribution was divided into peripheral and central distributions. Peripheral distribution was defined as being located in the outer third of the lung, while central distribution was defined as being limited to the inner two-thirds of the lung. Contrast enhancement was defined as attenuation difference with 20 Hounsfield units between pre-and post-contrast CT scans. The maximum SUVmax on ^{18}FDG-PET/CT was measured for the lung lesions, and the cut-off value for positive uptake was 2.5.

STATISTICAL ANALYSIS

Statistical analysis was performed using commercial statistical software (SPSS for Windows, version 23.0; IBM Corp., Armonk, NY, USA). A chi-squared test was used to analyze the ordinal data. CT images were analyzed by two radiologists in consensus (W.G.J., 11 years of experience;

J.E.L., 8 years of experience). Interobserver agreement for imaging patterns (nodular vs. consolidation), air-bronchogram, pleural tagging, and cavitation was assessed using a kappa value of agreement with 95% confidence intervals (CIs). Statistical significance was set at a *p*-value < 0.05.

RESULTS

The patient population consisted of 14 males and 17 females (mean age 60 years, range 19 to 78 years). Of the 31 patients, 24 (77.4%) were asymptomatic. In seven patients (22.6%), symptoms included cough (*n* = 6) and sputum production (*n* = 1). Nine patients had underlying solid malignancies, including breast, colorectal, gastric, ovarian, endometrial, lung, and thyroid cancer. All were in disease-free states at the time of diagnosis. The diagnosis of pulmonary crypto-

Table 1. Demographics and Clinical Informations of Patients with Pulmonary Cryptococcosis

Demographics	*n* (%)
Age, year	59.94 ± 13.73
Sex, female	17 (54.8)
Malignancy	9 (29.0)
DM	7 (22.6)
History of smoking	7 (22.6)
COPD	1 (3.2)
Presenting symptom	
Asymptomatic	24 (77.4)
Cough	6 (19.4)
Blood-tinged sputum	1 (3.2)
Laboratory Findings	**Mean ± SD**
WBC, × 10^9/L	6.93 ± 2.09
Hgb, g/L	13.1 ± 1.56
Platelet count, × 10^9/L	235.48 ± 66.04
C-reactive protein, mg/dL	0.28 ± 0.32
Serum cryptococcal antigen	
Positive	6 (19.4)
Negative	13 (41.9)
Not examined	12 (38.7)
Clinical Impression Before Pathologic Confirmation	***n* (%)**
Primary lung cancer	14 (45.2)
Pulmonary metastasis	9 (29.0)
Unresponsive pneumonia to empirical treatment	7 (22.6)
Benign tumor	1 (3.2)
Methods for Pathologic Confirmation	***n* (%)**
Surgical resection	19 (61.3)
TTNB	7 (22.6)
TBLB	5 (16.1)

COPD = chronic obstructive pulmonary disease, DM = diabetes mellitus, Hgb = hemoglobin, SD = standad deviation, TBLB = transbronchial lung biopsy, TTNB = transthoracic needle biopsy, WBC = white blood cell

coccosis was confirmed by surgical resection (*n* = 19), transthoracic needle biopsy (*n* = 7), and transbronchial lung biopsy (*n* = 5). Before the definite diagnosis of cryptococcosis had been determined, radiologic impressions before biopsy were performed, which included primary lung malignancies (*n* = 14), pulmonary metastases from an extra-thoracic solid malignancy (*n* = 9), pneumonia unresponsive to empirical treatment (*n* = 7), and benign tumors (*n* = 1) (Table 1).

The imaging findings of patients with pulmonary cryptococcosis were summarized in Tables 2 and 3. The nodule-dominant CT pattern were observed in 21 patients (21/31, 67.7%)

Table 2. Main Imaging Findings of Patients with Pulmonary Cryptococcosis

Major Imaging Patterns	*n* (%)
Nodule-dominant	21 (67.7)
Single nodular	14 (45.2)
Clustered nodular	4 (12.9)
Scattered nodular	3 (9.7)
Consolidation-dominant	10 (32.3)
Single lobe consolidation	6 (19.4)
Multi-lobes consolidation	4 (12.9)
Involvement and Distribution	***n* (%)**
Lobar involvement	
Single lobe	24 (77.4)
Multi-lobes	7 (22.6)
Distribution	
Upper	20 (64.5)
Non-upper	11 (35.5)
Peripheral	31 (100)
Central	0 (0)

Table 3. Ancillary Imaging Findings of Patients with Pulmonary Cryptococcosis

Ancillary Imaging Findings	*n* (%)
Ground-glass opacity component	2 (6.5)
Air bronchogram	14 (45.2)
Cavitation (or pseudocavitation)	7 (22.6)
Pleural tagging	7 (22.6)
Pleural effusion	2 (6.5)
Mediastinal lymphadenopathy	1 (3.2)
Degree of enhancement	
≥ 20 HU	22 (71)
< 20 HU	1 (3.2)
NA*	8 (25.8)
SUVmax on PET/CT	
≥ 2.5	10 (32.3)
< 2.5	7 (22.6)
Not examined	14 (45.2)

*Evaluation was impossible due to the small size or subsolid density of the lesion.
HU = Hounsfield unit, SUVmax = maximum standardized uptake value

and the consolidation-dominant CT pattern were observed in 10 patients (10/31, 32.3%). Among the patient with nodule-dominant CT pattern, the single nodular pattern was the most common pattern and was observed in 14 patients (14/31, 45.2%). It commonly presented as a nodule with well-defined margins (Fig. 1). The clustered nodular pattern was noted in four patients (4/31, 12.9%), mainly in the form of single lobe involvement with the peripheral distribution. The scattered nodular pattern was observed in three patients (3/31, 9.7%). The consolidation-dominant pattern was observed in 10 patients (32.3%). Among the patient with consolidation-dominant CT pattern, the single-lobe consolidation was observed in 6 patients (6/31, 19.4%) and multi-lobes consolidation was observed in 4 patients (4/31, 12.9%).

According to the involvement and distribution, 24 patients (77.4%) showed single-lobar involvement (Fig. 2), while the remaining 7 (22.6%) showed multi-lobar involvement (Fig. 3). When the lesions were divided by the distribution of the dominant lesion, 20 patients (64.5%) showed upper distribution, while all patients (100%) showed peripheral distribution.

The most common ancillary imaging finding was air bronchograms (45.2%). Cavitation was observed in seven patients (22.6%). Pleural tagging was observed in seven patients (22.6%). Ground-glass opacity components were observed in two patients (6.5%), which were accompanied by consolidation. Only one patient presented with pleural effusion and medi-

Fig. 1. Pulmonary cryptococcosis in a 76-year-old male.
A-C. Axial high-resolution CT scan reveals a peripheral solid nodule with pleural tagging in the right lower lobe (A). Axial pre-and post-contrast CT scans reveal contrast enhancement (more than 20 Hounsfield Units) of the solid nodule (B, C).
D. PET/CT scan demonstrates high ^{18}fluorodeoxyglucose uptake (maximum standardized uptake value, 6.6), mimicking a malignant tumor.

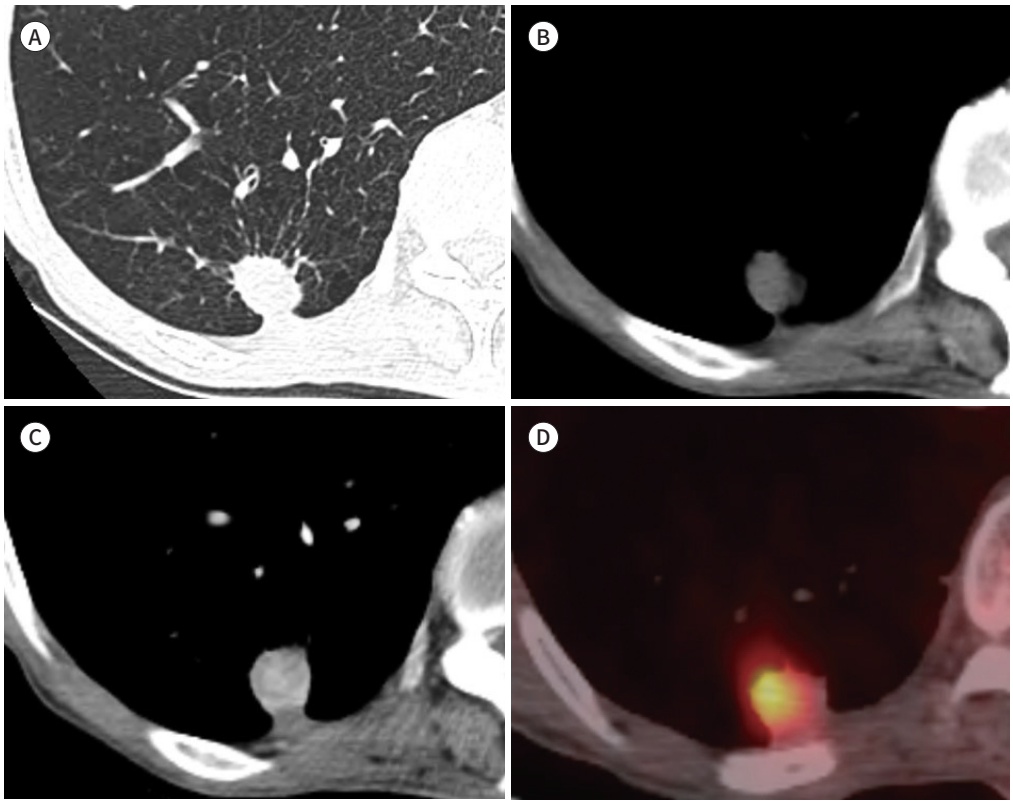

Fig. 2. Pulmonary cryptococcosis in a 67-year-old female.
A. Axial high-resolution CT scan at the level of the carina reveals consolidation with an air bronchogram (arrow) in the right upper lobe. A pathological diagnosis was made following a transbronchial lung biopsy, and the serum cryptococcal antigen test was positive.
B. After 5 months of treatment with fluconazole, an axial high-resolution CT scan reveals marked improvement.

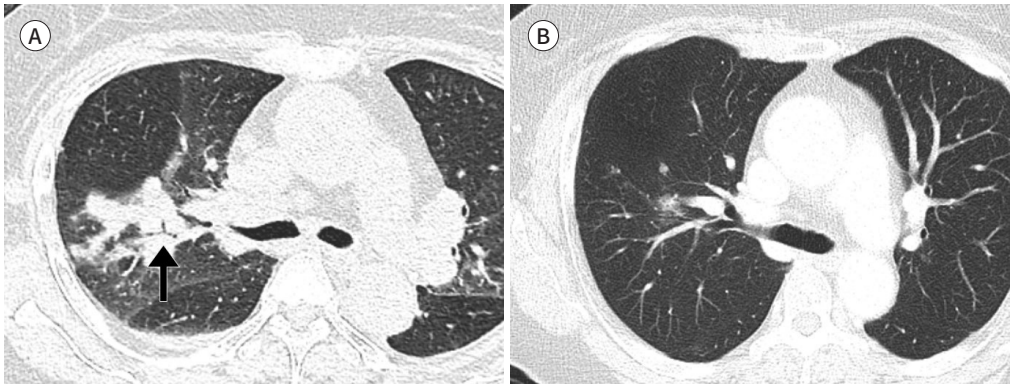

Fig. 3. Pulmonary cryptococcosis in a 40-year-old male.
A, B. An axial high-resolution CT scan reveals subpleural consolidation with perilesional ground-glass opacities (halo sign) in the left lower lobe at different levels.
C. A coronal reconstruction image reveals multi-lobar involvement and consolidation with an air bronchogram in the left lower lobe (arrows).

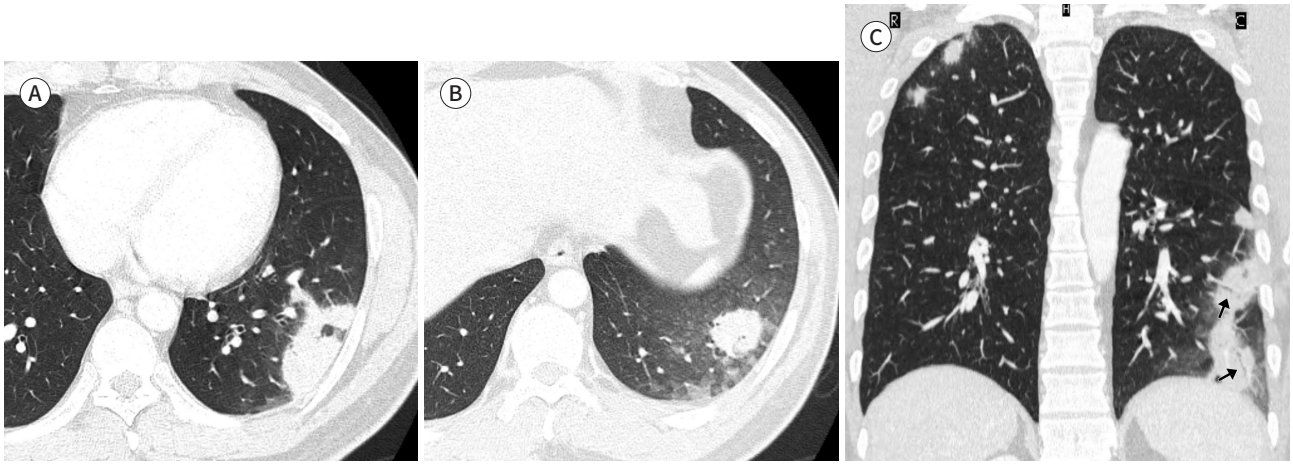

astinal lymphadenopathy (3.2%). Not all patients could be evaluated with contrast enhancement as eight patients (25.8%) had small sizes of lesions or sub-solid densities. Contrast enhancement was observed in 22 patients (22/23, 95.7%). ^{18}FDG-PET/CT was performed in 17 patients, and positive uptake was observed in 10 patients (10/17, 58.8%).

Substantial agreement between two radiologists was demonstrated for classification of imaging patterns (κ = 0.73; 95% CI, 0.50–0.97; p < 0.001), air bronchograms (κ = 0.75; 95% CI, 0.52–0.97; p < 0.001), pleural tagging (κ = 0.82; 95% CI, 0.58–1.06; p < 0.001), and cavitation (κ = 0.912; 95% CI, 0.74–1.08; p < 0.001).

Serum CrAg test was performed in 19 patients. The presence of serum CrAg was observed in six patients (6/19, 31.6%), which was significantly associated with the consolidation-dominant pattern (p = 0.011) (Table 4).

Substantial agreement between two radiologists was demonstrated for classification of im-

Table 4. CrAg Test Results Depending on Imaging Findings

Variables	CrAg (+) (*n* = 6)	CrAg (-) (*n* = 13)	*p*-Value
Extent of lesion			0.320
Single lobe	3 (50)	10 (76.9)	
Multi-lobes	3 (50)	3 (23.1)	
Imaging pattern			0.011
Nodule dominant	0 (0)	9 (69.2)	
Consolidation dominant	6 (100)	4 (30.8)	
Ground-glass opacity component	1 (16.7)	1 (7.7)	0.554
Air-bronchogram	5 (83.3)	6 (46.2)	0.177
Cavitation (or pseudocavitation)	3 (50)	3(23.1)	0.320
Pleural tagging	0 (0)	4 (30.8)	0.255
Pleural effusion	2 (33.3)	0 (0)	0.088
Mediastinal lymphadenopathy	1 (16.7)	0 (0)	0.316
Enhancement (≥ 20 HU)	5 (83.3)	9 (69.2)	0.516

Values in parentheses are percentages.
CrAg = cryptococcal antigen, HU = Hounsfield unit

aging patterns (κ = 0.73; 95% CI, 0.50–0.97; $p < 0.001$), air bronchograms (κ = 0.75; 95% CI, 0.52–0.97; $p < 0.001$), pleural tagging (κ = 0.82; 95% CI, 0.58–1.06; $p < 0.001$), and cavitation (κ = 0.912; 95% CI, 0.74–1.08; $p < 0.001$).

DISCUSSION

The diagnosis of pulmonary cryptococcosis is based on isolation of cryptococcus spores or detection of cryptococcal antigens in a pulmonary specimen (11). Diagnostic therapy and lung biopsy are usually used in the diagnosis of pulmonary cryptococcosis. However, these tools have some disadvantages. For example, diagnostic therapy can yield adverse drug effects and requires a long time to achieve a definite diagnosis of pulmonary cryptococcosis and tissue biopsy is also an invasive procedure. As a non-invasive method, therefore, serum CrAg test is widely used for diagnosing pulmonary cryptococcosis.

It was reported that the presence of serum CrAg was more frequently observed among patients with extensive pulmonary involvement or multi-lobar involvement (9, 12). In our study, similar results were obtained in the consolidation dominant CT pattern rather than the nodule dominant CT pattern, but there was no significant difference in serum CrAg test results in multiple lesions and multi-lobar involvement. These may imply that if focal pneumonic consolidation has not been improved by antibiotics, serum CrAg test might be helpful in diagnosing pulmonary cryptococcosis.

In addition, according to one study, it was reported that pulmonary cryptococcus spontaneously resolves in immunocompetent hosts over a period of one year or more without any specific complications and with/without appropriate antifungal treatment (13). However, as the nodular pattern mimics lung cancer and is difficult to differentiate radiologically if the life expectancy of a person who is misdiagnosed with cancer is long, simple follow-up observation for a long period without biopsy or surgical treatment will be rare.

Pulmonary cryptococcosis can be presented as various imaging findings. In previous studies, it has been reported that the multiple nodular lesions were the most common pattern. However, the single nodular pattern was the most common pattern of lung lesion in our study. This is thought to be because the single nodular pattern was more difficult to discriminate from a primary lung malignancy than other patterns, in which case invasive procedures might be performed more aggressively (5, 7).

23 (74.2%) patients were thought as primary lung cancer or metastasis at initial imaging studies (Table 1). Contrast enhancement and high FDG uptake on ^{18}FDG-PET/CT often leads to initial clinical misdiagnosis of malignancy, especially when lung lesions appeared as nodular patterns. In immunocompetent patients, pulmonary cryptococcosis is commonly demonstrated as pulmonary nodules and may not be accurately differentiated from cancer on the basis of showing contrast enhancement or high uptake on ^{18}FDG-PET/CT (4, 5, 8).

Of the 10 patients with consolidation-dominant CT pattern, seven patients were firstly diagnosed with pneumonia as the initial radiologic impression. However, two patients had a mild cough without acute symptoms of pneumonia, and other eight patients had no symptoms. Pulmonary cryptococcosis in the immunocompetent patients is often asymptomatic and has mild symptoms rather than severe symptoms such as respiratory failure (1, 9).

This study has several limitations. First, it was a single-center retrospective study and the disease has a very low prevalence in immunocompetent patients, so the number of cases included was small. Second, there may be selection bias because serum CrAg tests were selectively performed according to the decision of clinicians. For generalization, further research using a larger sample size is needed.

In conclusion, combination of CT findings showing consolidation and serum cryptococcal antigen test may be helpful for diagnosing pulmonary cryptococcosis in immunocompetent patient.

Author Contributions

Conceptualization, all authors; data curation, C.H.S.; formal analysis, C.H.S., L.J.E., P.H.M.; investigation, C.H.S.; methodology, C.H.S., K.Y., J.W.G., L.J.E.; project administration, K.Y.; supervision, K.Y., J.W.G., L.J.E.; validation, K.Y., J.W.G., L.J.E., P.H.M.; visualization, K.Y., J.W.G., L.J.E., P.H.M.; writing—original draft, C.H.S.; and writing—review & editing, J.W.G.

Conflicts of Interest

Yun-Hyeon Kim has been a Editorial Board Member of the Journal of the Korean Society of Radiology since 2002; however, he was not involved in the peer reviewer selection, evaluation, or decision process of this article. Otherwise, no other potential conflicts of interest relevant to this article were reported.

Funding

None

REFERENCES

1. Setianingrum F, Rautemaa-Richardson R, Denning DW. Pulmonary cryptococcosis: a review of pathobiology and clinical aspects. *Med Mycol* 2019;57:133-150
2. Khoury MB, Godwin JD, Ravin CE, Gallis HA, Halvorsen RA, Putman CE. Thoracic cryptococcosis: immunologic competence and radiologic appearance. *AJR Am J Roentgenol* 1984;142:893-896
3. Patz EF Jr, Goodman PC. Pulmonary cryptococcosis. *J Thorac Imaging* 1992;7:51-55

4. Lindell RM, Hartman TE, Nadrous HF, Ryu JH. Pulmonary cryptococcosis: CT findings in immunocompetent patients. *Radiology* 2005;236:326-331
5. Fox DL, Müller NL. Pulmonary cryptococcosis in immunocompetent patients: CT findings in 12 patients. *AJR Am J Roentgenol* 2005;185:622-626
6. Zhang Y, Li N, Zhang Y, Li H, Chen X, Wang S, et al. Clinical analysis of 76 patients pathologically diagnosed with pulmonary cryptococcosis. *Eur Respir J* 2012;40:1191-1200
7. Zinck SE, Leung AN, Frost M, Berry GJ, Müller NL. Pulmonary cryptococcosis: CT and pathologic findings. *J Comput Assist Tomogr* 2002;26:330-334
8. Kishi K, Homma S, Kurosaki A, Kohno T, Motoi N, Yoshimura K. Clinical features and high-resolution CT findings of pulmonary cryptococcosis in non-AIDS patients. *Respir Med* 2006;100:807-812
9. Min J, Huang K, Shi C, Li L, Li F, Zhu T, et al. Pulmonary cryptococcosis: comparison of cryptococcal antigen detection and radiography in Immunocompetent and Immunocompromised patients. *BMC Infect Dis* 2020;20:91
10. Hansell DM, Bankier AA, MacMahon H, McLoud TC, Müller NL, Remy J. Fleischner Society: glossary of terms for thoracic imaging. *Radiology* 2008;246:697-722
11. Jarvis JN, Harrison TS. Pulmonary cryptococcosis. *Semin Respir Crit Care Med* 2008;29:141-150
12. Zhu T, Luo WT, Chen GH, Tu YS, Tang S, Deng HJ, et al. Extent of lung involvement and serum cryptococcal antigen test in non-human immunodeficiency virus adult patients with pulmonary cryptococcosis. *Chin Med J (Engl)* 2018;131:2210-2215
13. Fisher JF, Valencia-Rey PA, Davis WB. Pulmonary cryptococcosis in the immunocompetent patient-many questions, some answers. *Open Forum Infect Dis* 2016;3:ofw167

정상 면역 환자에서 폐 크립토코쿠스증의 임상방사선학적 특징

최홍석[1] · 김윤현[1,2*] · 정원기[3] · 이종은[1] · 박혜미[1]

목적 정상 면역 환자에서 폐 크립토코쿠스증의 컴퓨터단층촬영 영상 소견과 임상 양상에 대하여 분석해 보고자 하였다.

대상과 방법 2008년 1월부터 2019년 11월까지 흉부 컴퓨터단층촬영을 시행하였으며, 조직병리학적 검사로 진단된 정상 면역 폐 크립토코쿠스 환자를 대상으로 후향적 분석을 시행하였다. 영상 소견은 주 영상 형태, 병변의 분포, 보조적 영상 소견으로 구분하였다. 혈청 크립토코쿠스 항원의 유무에 따른 임상 및 방사선학적 특징을 확인하기 위해 단변수 분석을 시행하였다.

결과 총 31명의 환자를 분석하였다(평균 연령: 60세, 범위 19–78세). 단일 폐엽에 국한된 단일 결절성 병변이 가장 흔한 주된 영상 소견이었다(14/31, 45.2%). 19명의 환자에서 혈청 크립토코쿠스 항원 검사를 시행하였다(19/31, 61.3%). 6명의 환자에서 혈청 크립토코쿠스 항원이 검출됐으며(6/19, 31.6%), 이들 모두 폐경결 우세 형태를 보였다. 혈청 크립토코쿠스 항원은 결절 우세 형태보다 폐경결 우세 형태에서 보다 유의미하게 검출되었다($p = 0.011$).

결론 폐경결 형태의 CT 영상 소견을 보이고 혈청 크립토코쿠스 항원 검사가 양성을 보이는 조합은 정상 면역 폐 크립토코쿠스 환자의 진단에 도움이 될 수 있다.

[1]전남대학교병원 영상의학과,
[2]전남대학교 의과대학 영상의학교실,
[3]화순전남대학교병원 영상의학과